August 22, 2025

Big Bang Nucleosynthesis: Deuterium Production in the Early Universe

Fatih Žgalj,[1] Supervisors: Miguel Escudero Abenza,[2] and Maksym Ovchynnikov[2]

[1] *University of Sarajevo*
[2] *CERN*

ABSTRACT

Through the concordance model of cosmology, it is possible to predict the primordial abundances of light elements within the framework of Big Bang Nucleosynthesis (BBN). These predictions agree remarkably well with observations of the primordial abundances of helium-4 and deuterium. Specifically, the deuterium abundance is strongly sensitive to nuclear reaction rates, such as $\mathrm{D}+\mathrm{D}\to {}^3\mathrm{He}+n$ or $\mathrm{D}+\mathrm{D}\to \mathrm{T}+p$. By understanding how the abundances depend on variations to relevant parameters and reaction rates, we hope to improve our knowledge of them to allow stronger cosmological inferences to be made from deuterium observations. These in turn allow us to make important improvements in estimating cosmological parameters such as N_{eff}, the effective number of neutrino species.

1. THE EXPANDING UNIVERSE

The success of the Big Bang model of the Universe is in great part due to the remarkable agreement between theoretical predictions and astronomical observations, to name a few: expansion of the universe as described by Hubble's law, light element abundances in accordance with BBN predictions, and anisotropies in the cosmic microwave background (CMB). In order to explain certain phenomena, however, one must accept several beyond-the-Standard-Model constituents, namely dark matter and dark energy, as well as a mechanism for generating perturbations in the early universe (often dubbed inflation).

In 1929, Edwin Hubble formulated what is now referred to as the Hubble-Lemaître law. Even before that, in 1922, Alexander Friedmann showed that general relativity predicts an expanding universe. Hubble found that all galaxies were receding from us, i.e. the light coming from them was redshifted. Furthermore, the velocity at which they are receding increases with distance. The amount of evidence gathered until this day (Fig. 8) has now solidified this theory.

In order to quantify the expansion of the universe, we introduce a dimensionless scale factor a, defined as the ratio of the physical distance between two points and their comoving distance[3]. and set its present value to 1. Equivalently, one can express the expansion of the universe through the redshift factor z:

$$1+z\equiv\frac{\lambda_{\mathrm{obs}}}{\lambda_{\mathrm{emit}}}=\frac{a_{\mathrm{obs}}}{a_{\mathrm{emit}}}=\frac{1}{a_{\mathrm{emit}}}\,. \tag{1.1}$$

We have good reason to believe our universe is, to good approximation, flat (Euclidean). Einstein's general relativity provides a link between the geometry of space and its energy content. Therefore, it allows us to track the evolution of the scale factor with time, depending on what the dominant ingredient in the energy density was at a certain time. For example, a radiation-dominated universe has $a\propto t^{1/2}$; for a matter-dominated universe, $a\propto t^{2/3}$; and recently, the trend has been exponential, suggesting a new constituent beginning to dominate: dark energy. To describe this change in the scale factor, we introduce the Hubble rate

$$H(t)\equiv\frac{1}{a}\frac{\mathrm{d}a}{\mathrm{d}t}\,. \tag{1.2}$$

If the comoving distance between two points is x, their physical distance thus being $d=ax$, in absence of comoving motion ($\dot{x}=0$), the relative velocity is

[3] By comoving distance we assume the distance between points on a grid which expands with the space, such that the difference between coordinates—the comoving distance—remains constant.

$$v = \frac{\mathrm{d}}{\mathrm{d}t}(ax) = \dot{a}x = H_0 d \; (v \ll c)\,, \tag{1.3}$$

where H_0 denotes the value of the Hubble rate today and is also known as Hubble's constant. Eq. (1.3) represents the Hubble-Lemaître law. The Hubble constant is usually written in terms of a dimensionless parameter h (not to be confused with Planck's constant) as

$$H_0 = 100h\,\mathrm{km\,s^{-1}\,Mpc^{-1}}\,. \tag{1.4}$$

Current measurements give $h \simeq 0.7$.

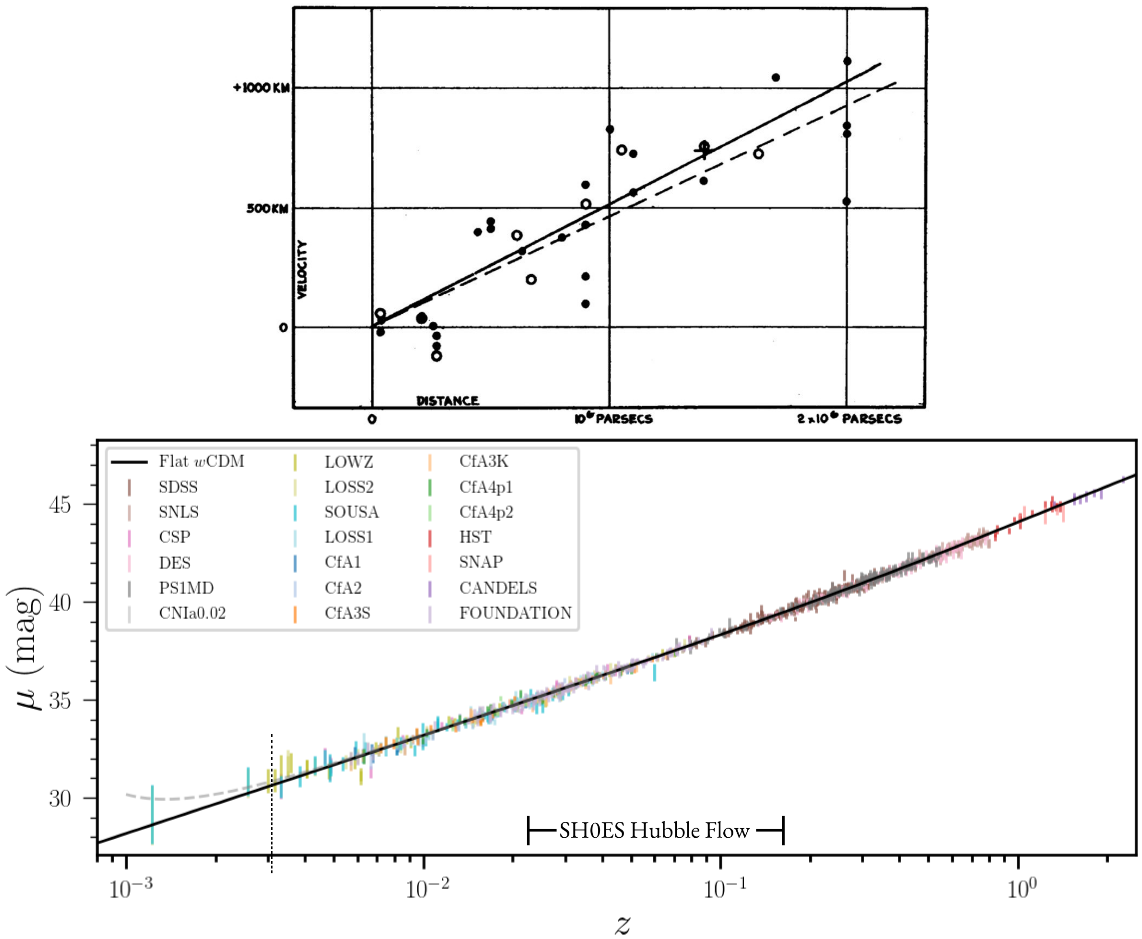

Figure 1. *Top:* Hubble's original diagram from 1929 shows the "velocity-distance relation among 'extra-galactic nebulae'" (i.e. galaxies). Taking into account that the y-axis should be labeled as $\mathrm{km\,s^{-1}}$, it is easy to infer $H_0 \simeq 500\,\mathrm{km\,s^{-1}\,Mpc^{-1}}$, off by an order of magnitude from the accepted value today. *Bottom:* A modern version of the Hubble diagram by The Pantheon+ Analysis (D. Brout et al. 2022). The part of the graph to the left of the dashed line corresponds to the range of Hubble's original diagram above.

More generally, the dependence of H is given by Friedmann's equations (derived from general relativity), the first one being:

$$H^2(t) = \frac{8\pi G}{3}\left[\rho(t) + \frac{\rho_{\mathrm{cr}} - \rho(t_0)}{a^2(t)}\right]\,, \tag{1.5}$$

where G is the well-known Newton's gravitational constant, $\rho(t)$ is the energy density in the universe (with $\rho(t_0)$ being its present value), and ρ_{cr} is the critical density. The second term in the equation represents the curvature contribution and scales as $1/a^2$. If this term vanishes (in a flat universe), that means we should measure the energy density today to be equal to the critical density

$$\rho_{\rm cr} \equiv \frac{3H_0^2}{8\pi G}\,, \tag{1.6}$$

which, to within errors, seems to be the case in all observations (and is on the order of $10^{-29}\,\mathrm{g\,cm^{-3}}$. We will therefore confine our analysis to a Euclidean universe.

A keen observer will notice that the Friedmann equation is useful only if the evolution of the energy density as a function of time is known. This, however, is not a trivial thing and one should first consider separately several different constituents.

For nonrelativistic matter, the energy of a particle is essentially equal to its rest mass energy and thus remains constant with time. Due to the expansion of the universe (one can imagine an expanding box with particles inside) and the number density being inversely proportional to the volume, the energy density of nonrelativistic matter scales as a^{-3}.

Another key ingredient of our universe is the radiation which permeates it in the form of photons and which we measure today as the cosmic microwave background (CMB). In the hot and dense early universe, photons interacted with other particles, for example by ionizing any nuclei, and later atoms that may have formed. At some later time, known as the recombination epoch, with temperature of about 0.3 eV (corresponding to order of $10^4\,\mathrm{K}$), somewhat lower than the binding energy of hydrogen (13.6 eV), electrons and protons formed hydrogen atoms[4]. After that, photons in the primordial soup stopped interacting and were able to travel freely. Having been in thermal equilibrium before this, the spectrum of the photons we measure today follows a perfect black-body distribution with a temperature of $T_0 = 2.726 \pm 0.001\,\mathrm{K}$ (D. J. Fixsen 2009). By looking at these photons, we are essentially getting a glimpse into the universe as it was some 380,000 years ago. Measurements show a high degree of isotropy in the CMB, but the small density perturbations (of order 10^{-5}) gave rise to the structure we see in the universe today.

The wavelength of these photons is "stretched" with the expansion of the universe ($\lambda \propto a$) which means their energy scales as $1/a$. The volume increasing by a factor of a^3, this means that the energy density of (black-body) radiation scales as a^{-4}. Another way to see this is to recall that the black-body spectrum is a function of ν/T, so instead of taking the frequency to scale with a, one can equivalently say that the temperature of radiation changes as $T(t) = T_0/a(t)$. From the well-known Stefan-Boltzmann law, we know the energy density scales as $T^4 \propto a^{-4}$. Making use of Eq. (1.5), we see that at early times, $H \propto T^2$.

Finally, dark energy is introduced to the energy budget of the universe through a cosmological constant Λ, which implies that its energy density remains constant over time. Whether this is entirely true, however, remains an open question.

2. ENERGY CONTENT OF THE UNIVERSE

In a smooth and isotropic universe, the energy-momentum tensor which goes into the Einstein equations assumes a very simple form:

$$T^{\mu}{}_{\nu} = \begin{pmatrix} -\rho & 0 & 0 & 0 \\ 0 & \mathcal{P} & 0 & 0 \\ 0 & 0 & \mathcal{P} & 0 \\ 0 & 0 & 0 & \mathcal{P} \end{pmatrix} \tag{2.1}$$

where $\mathcal{P}$ is the pressure. This is in fact the energy-momentum tensor of an ideal fluid at rest. With that analogy in mind, and using the continuity equation $\partial\rho/\partial t = 0$ as well as the Euler equation $\partial\mathcal{P}/\partial x^i = 0$, it is possible to write a general-relativistic version by requiring the covariant derivative to vanish:

$$\boldsymbol{\nabla}_{\mu} T^{\mu}{}_{\nu} = 0\,. \tag{2.2}$$

[4] This being the first time it happened, the prefix 're-' seems unnecessary.

From here follows the conservation law in an expanding universe:

$$\frac{\partial\rho}{\partial t}+\frac{\dot{a}}{a}\left[3\rho+3\mathcal{P}\right]=0\,, \tag{2.3}$$

or, rearranging terms:

$$a^{-3}\frac{\partial(\rho a^3)}{\partial t}=-3\frac{\dot{a}}{a}\mathcal{P}\,. \tag{2.4}$$

Throughout the early universe, most reactions proceeded rapidly enough to keep particles in equilibrium (sharing the same temperature). When considering the evolution of the abundance of a certain species, then, it will be useful to have expressions for the energy density and pressure in terms of temperature:

$$\rho_s=g_s\int\frac{\mathrm{d}^3p}{(2\pi)^3}f_s(\mathbf{x},\mathbf{p})E(p) \tag{2.5}$$

and

$$\mathcal{P}_s=g_s\int\frac{\mathrm{d}^3p}{(2\pi)^3}f_s(\mathbf{x},\mathbf{p})\frac{p^2}{3E(p)}\,. \tag{2.6}$$

Here the subscript s denotes a species, g_s is the degeneracy and $f_s(\mathbf{x},\mathbf{p})$ is the distribution function of the species (Fermi-Dirac or Bose-Einstein):

$$f_{\mathrm{FD/BE}}=\frac{1}{e^{(E-\mu)/T}\pm1} \tag{2.7}$$

which in general depends on the position $\mathbf{x}$ and momentum $\mathbf{p}$ of the particle.[5]

Consider now several constituents of the universe, similar to what was done in the previous chapter. For nonrelativistic matter, the pressure is effectively equal to zero, so $\partial\rho_{\mathrm{m}}a^3/\partial t=0$, and the energy density of matter scales as $\rho_{\mathrm{m}}\propto a^{-3}$. Considering the discussion in the previous chapter, this is not a surprising result. In the case of radiation, $\mathcal{P}_{\mathrm{r}}=\rho_{\mathrm{r}}/3$, which when inserted in Eq. (2.3) gives

$$\frac{\partial\rho_{\mathrm{r}}}{\partial t}+\frac{\dot{a}}{a}4\rho_{\mathrm{r}}=a^{-4}\frac{\partial(\rho_{\mathrm{r}}a^4)}{\partial t}=0\,, \tag{2.8}$$

which means that $\rho_{\mathrm{r}}\propto a^{-4}$.

It is convenient to introduce the *equation of state* parameter of a species as

$$w_s=\frac{\mathcal{P}_s}{\rho_s}\,. \tag{2.9}$$

For example, matter has $w_{\mathrm{m}}=0$, radiation $w_{\mathrm{r}}=1/3$, and the cosmological constant (dark energy) has $w_\Lambda=-1$. However, because the equation of state is not time-independent in general, a more accurate description of the evolution of a species s can be obtained by integrating Eq. (2.3) with $w_s=w_s(a)$:

$$\rho_s(a)\propto\exp\left\{-3\int^a\frac{\mathrm{d}a'}{a'}\left[1+w_s(a')\right]\right\}. \tag{2.10}$$

For time-independent w_s, the expression reduces to $\rho_s(a)\propto a^{-3(1+w_s)}$.

The chemical potential μ appearing in the distribution function is for almost all particles at almost all times very small compared to the temperature. Then the distribution function only depends on E/T and it can be shown that the pressure satisfies

$$\frac{\partial\mathcal{P}_s}{\partial T}=\frac{\rho_s+\mathcal{P}_s}{T}\,. \tag{2.11}$$

Eq. 2.4 can be rewritten as

$$a^{-3}\frac{\partial\left[(\rho+\mathcal{P})a^3\right]}{\partial t}-\frac{\partial\mathcal{P}}{\partial t}=0\,. \tag{2.12}$$

[5] Here $\mathbf{p}$ is the proper momentum, not the comoving momentum.

Since by the chain rule $\partial\mathcal{P}/\partial t = \mathrm{d}T/\mathrm{d}t\ \partial\mathcal{P}/\partial T$,

$$a^{-3}\frac{\partial\left[(\rho+\mathcal{P})a^3\right]}{\partial t} - \frac{\mathrm{d}T}{\mathrm{d}t}\frac{\rho+\mathcal{P}}{T} = a^{-3}\,T\frac{\partial}{\partial t}\left[\frac{(\rho+\mathcal{P}a^3}{T}\right] = 0\,. \tag{2.13}$$

We see that the entropy density

$$s \equiv \frac{\rho+\mathcal{P}}{T} \tag{2.14}$$

scales as a^{-3}. This holds for the total entropy of all species regardless of whether they are in equilibrium, as well as individual species (even with nonzero chemical potential).

Finally, it is useful to define the *density parameters* as the ratio of the energy density of a species to the critical density (Eq. (1.6)) today:

$$\Omega_s \equiv \frac{\rho_s(t_0)}{\rho_{\mathrm{cr}}}\,. \tag{2.15}$$

Therefore, the evolution of energy density is described by

$$\rho_s(a) = \Omega_s\rho_{\mathrm{cr}}a^{-3(1+w_s)}\,, \tag{2.16}$$

if the equation of state is time-independent. In Chapter 1 it was emphasized that H_0 is not precisely known, so the densities are usually expressed in terms of a quantity $\omega_s \equiv \Omega_s h^2$.

2.1. *Photons*

For photons, the energy density is given by ($g_\gamma = 2$ for the two spin states of the photon):

$$\rho_\gamma = 2\int\frac{\mathrm{d}^3p}{(2\pi)^3}\frac{p}{e^{p/T}-1}\,. \tag{2.17}$$

The chemical potential is equal to zero because in the early universe, photon number is not conserved.[6] Making use of the Riemann zeta function, the final result is

$$\rho_\gamma = \frac{\pi^2}{15}T^4\,. \tag{2.18}$$

It follows that the photon density parameter today is

$$\Omega_\gamma h^2 = 2.47\cdot 10^{-5}\,. \tag{2.19}$$

2.2. *Baryons*

Cosmologists usually refer to all nuclei and electrons as *baryons*. Because the nuclei are much more massive than the electrons, practically all of the mass is in the actual baryons. Baryons, however, cannot be described by an equilibrium distribution function. We must therefore rely on direct measurements. The abundance of light elements formed during BBN gives a constraint on $\Omega_{\mathrm{b}}h^2$, with deuterium being the most sensitive to the baryon density. Measurements of the fractional amount of deuterium in high-redshift absorption systems yield $\Omega_b h^2 = 0.0222 \pm 0.0005$ (R. J. Cooke et al. 2018). There are also other methods that constrain the baryon density by, for example, looking at anisotropies in the CMB.

The baryon density determined from this makes up only about 5% of the critical density today. However, astronomical measurements (galaxy velocities, gravitational lensing, etc.) have placed the total matter density at a value some 6 times larger than this, which means that more than 80% of the matter in the universe is non-baryonic.

[6] CMB observations place a limit on the chemical potential of $\mu/T < 9\cdot 10^{-5}$ (D. J. Fixsen et al. 1996).

2.3. *Neutrinos*

Throughout these notes, we will consider only the three generations of neutrinos in the Standard Model, but sometimes replace the number 3 with N_ν (number of neutrino species) to emphasize the dependence of a certain quantity on it. There is one spin degree of freedom for each neutrino (left-handed) and one for each antineutrino (right-handed).

In the approximation of massless neutrinos, we can reuse the integral for the photon energy density, changing the denominator to $e^{p/T}+1$ (for fermions) and the prefactor to 6. The integral turns out to be a factor of 7/8 smaller than the one for photons:

$$\rho_\nu = 3 \cdot \frac{7}{8} \cdot \left(\frac{T_\nu}{T}\right)^4 \rho_\gamma \,. \tag{2.20}$$

The neutrino temperature T_ν will be different from the photon (EM plasma) temperature T.

At very early times, neutrinos were kept in equilibrium together with the rest of the cosmic plasma through weak interactions such as $e^-\nu_e \to \nu_e e^-$ or $e^+e^- \to \nu_e\nu_e$. The interactions being very weak, they eventually decoupled from the plasma and "froze out". This happened slightly before the temperature was of order of electron mass. After the temperature dropped below this, electrons and positrons began to annihilate, but none of this energy went into heating the neutrinos. We therefore expect the photons, which acquired the majority of the energy released during annihilation, to be hotter than the neutrinos.

We already mentioned that photons decoupled at temperature around 0.3 eV. Neutrinos, as we shall see, stopped interacting with the plasma at around 2–3 MeV, placing the temperature of cosmic neutrino background today at 1.95 K. However, these so-called relic neutrinos are notoriously difficult to detect and there has been no experimental success in that regard so far.

To take into account the annihilation of electrons and positrons, we use the fact that the total entropy density s scales as a^{-3}. From Eq. (2.14) we have for different massless species

$$s_s = \begin{cases} g_s \dfrac{2\pi^2}{45} T_s^3 \quad \text{(bosons)}\,, \\[2ex] \dfrac{7}{8} \cdot g_s \dfrac{2\pi^2}{45} T_s^3 \quad \text{(fermions)}\,. \end{cases} \tag{2.21}$$

Particles whose mass are significantly larger than the temperature at that time have a negligible contribution. Before e^+e^- annihilation, at $a=a_1$ and common temperature T_1:

$$\begin{aligned} s(a_1) &= \frac{2\pi^2}{45} T_1^3 \left[2 + \frac{7}{8}(4+6)\right] \\ &= \frac{43\pi^2}{90} T_1^3 \,. \end{aligned} \tag{2.22}$$

After annihilation, the electrons and positrons are almost fully gone, but now the temperatures of neutrinos and photons are not the same:[7]

$$s(a_2) = \frac{2\pi^2}{45}\left[2T^3 + \frac{7}{8}6T_\nu^3\right] \,. \tag{2.23}$$

Multiplying (2.22) by a_1^3 and (2.23) by a_2^3 and equating:

$$\frac{43}{2}(a_1T_1)^3 = 4\left[\left(\frac{T}{T_\nu}\right)^3 + \frac{21}{8}\right]_{a_2} (T_\nu(a_2)a_2)^3 \,. \tag{2.24}$$

Since neutrinos received a negligible amount of energy from the annihilation, their temperature always scales as a^{-1} (so $a_1T_1 = a_2T_\nu(a_2)$), leading to

$$\frac{T_\nu}{T} = \left(\frac{4}{11}\right)^{1/3} \,, \tag{2.25}$$

[7] Throughout these notes, we assume a common temperature for all neutrino species, i.e. $T_{\nu_e} = T_{\nu_\mu} = T_{\nu_\tau} \equiv T_\nu$, and also assume $T_\gamma = T_e$. The latter is a good approximation due to frequent scatterings between photons, electrons and positrons. The former is based on the fact that ν_μ and ν_τ have the same interactions in the Standard Model, as well as the presence of neutrino oscillations (which start at temperatures around 3–5 MeV) and have the effect of equilibrating the flavor distribution function.

which continues to hold until today. The neutrino density is then, from Eq. (2.20),

$$\rho_\nu = 3 \cdot \frac{7}{8} \cdot \left(\frac{4}{11}\right)^{1/3} \rho_\gamma \,. \tag{2.26}$$

From Eqs. (2.22) and (2.23) we see that the effective number of relativistic degrees of freedom g_* is $43/4 = 10.75$ before and $43/11 \simeq 3.909$ after annihilation.

Because neutrinos are not massless (we know this from observed neutrino oscillations), a refined approach is needed. For a single species of massive neutrino we have:

$$\rho_{\nu_i} = 2 \int \frac{\mathrm{d}^3 p}{(2\pi)^3} \frac{1}{e^{p/T_\nu}+1} \sqrt{p^2 + m_{\nu_i}^2} \,. \tag{2.27}$$

where $i = e, \mu, \tau$. In the high-temperature limit, Eq. (2.27) reduces to 1/3 of Eq. (2.26).

3. BIG BANG NUCLEOSYNTHESIS

This is the earliest epoch of the evolution of our universe that we can probe and analyze both theoretically and observationally and spans from temperature $T \sim 1\,\mathrm{MeV}$ and times of $t \sim 1\,\mathrm{s}$ to just below $T \sim 0.1\,\mathrm{MeV}$ and around $t \sim 3\,\mathrm{min}$ after the Big Bang (Fig. 2). The overall good agreement of predictions with abundance measurements and observations means that BBN is a very useful tool for checking and constraining new physics by calculating the influence of BSM theories on the known abundances. In that sense, it serves as a nice obstacle course for any proposed theories in the sense that they must pass the BBN test, that is, the changes they introduce must still match the observations.[8]

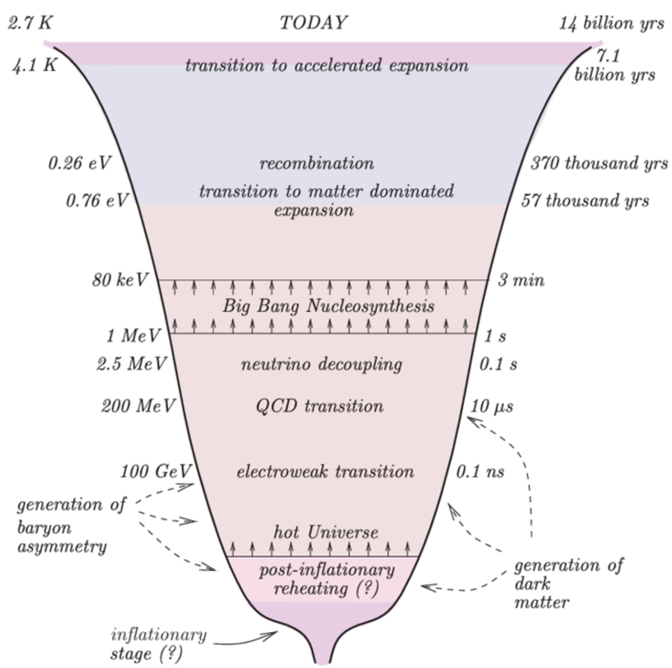

Figure 2. The evolution of the universe with some of the most important events marked on the time and temperature scale. From V. A. Rubakov & D. S. Gorbunov (2017).

[8] One can insert a hypothetical particle (such as a massive neutrino) and see what has to happen before BBN predicts abundances that are very different from observations. This has been done to put limits on the mass of a stable tau neutrino. From the viewpoint of the Standard Model, the importance of BBN boils down to the determination of a single parameter, baryon asymmetry η_b. BBN imposes limits on the density of new relativistic particles at $T \sim 1$ MeV. Also, there should be no decays or annihilations of new heavy particles with emission of hard photons at BBN epoch and somewhat later. If the main decay channel of a heavy particle X is $X \to Y\,\gamma$, where Y is a particle with $m_Y \ll m_X$, the energy of produced photon is $E_\gamma \approx m_X/2$. It is the emission of these photons that is dangerous because it leads to destruction of light elements, say deuterium or even helium-4.

Generally speaking, the abundances of light elements we measure today are the consequence of processes that occurred in the radiation-dominated epoch (at the mentioned temperature and age of the universe). The abundances are quite sensitive to what was going on in the universe at that time, some more so than others. Specifically, deuterium abundance is very sensitive to what was happening in the early universe.

Calculating these abundances precisely is not an easy task. A nice simplification is the fact that the physics splits up neatly into two parts, since, as we will see, above 0.1 MeV, no nuclei can form and only free protons and neutrons exist. We'll see the physical explanation behind this later. Therefore, the first step is to solve for the neutron to proton ratio and then use this abundance as input for the synthesis of nuclei.

3.1. *Neutron abundance*

The neutrons and protons in the primordial plasma are kept in equilibrium by weak interactions:

$$n \leftrightarrow p + e^- + \bar{\nu}_e \,, \tag{3.1}$$

$$n + \nu_e \leftrightarrow p + e^- \,, \tag{3.2}$$

$$n + e^+ \leftrightarrow p + \bar{\nu}_e \,. \tag{3.3}$$

In the early universe, the reactions proceed in both directions, which means that at high temperatures, there are roughly as many neutrons as protons. Besides them, the primordial plasma consists of photons, electrons/positrons and neutrinos, which decouple around 2–3 MeV as they interact very weakly. These neutrinos are the source of the predicted cosmic neutrino background (CNB).

If there had been no asymmetry in the initial number of baryons and antibaryons, then both would be completely depleted by 1 MeV. However, such an asymmetry has to exist, since otherwise we would observe a universe almost completely devoid of baryons. A useful parameter to describe this asymmetry is the ratio of baryons to photons, which changes slightly with the evolution of the universe, but is roughly 10^9 photons per baryon:

$$\eta_\mathrm{b} \equiv \frac{n_\mathrm{b}}{n_\gamma} = 6.0 \cdot 10^{-10} \left(\frac{\Omega_\mathrm{b} h^2}{0.022} \right) \,. \tag{3.4}$$

Therefore early universe is very much radiation-dominated, which helps simplify the equations of its evolution during that epoch.

A consequence of this is that at temperatures above 0.1 MeV, any nuclei that potentially form will be almost instantly broken apart by a photon from the high-energy tail of the Planck distribution, the photons being so much more abundant.

Fig. 3 shows the binding energy per nucleon.

It is convenient to introduce the ratio of the number density of neutrons to the number density of baryons as a new dimensionless quantity:

$$X_n = \frac{n_n}{n_p + n_n} \,. \tag{3.5}$$

Let us denote the rate of conversion of neutrons to protons by λ_{np}, and λ_{pn} for the conversion of protons to neutrons. The parameter of interest is the mass difference of neutrons and protons, $Q \equiv \Delta m \simeq 1.293\,\mathrm{MeV}$. As a good approximation, we can use the detailed balance principle which relates the direct and inverse rates in the high temperature limit:

$$\frac{\lambda_{p+e^- \to n+\nu_e}}{\lambda_{n+\nu_e \to p+e^-}} = e^{-Q/T} \,. \tag{3.6}$$

We can then write:

$$\frac{\mathrm{d}X_n}{\mathrm{d}t} = \lambda_{np} \left[(1 - X_n) e^{-Q/T} - X_n \right] \,. \tag{3.7}$$

To simplify the expressions, we introduce another dimensionless parameter

$$x = \frac{Q}{T} \,. \tag{3.8}$$

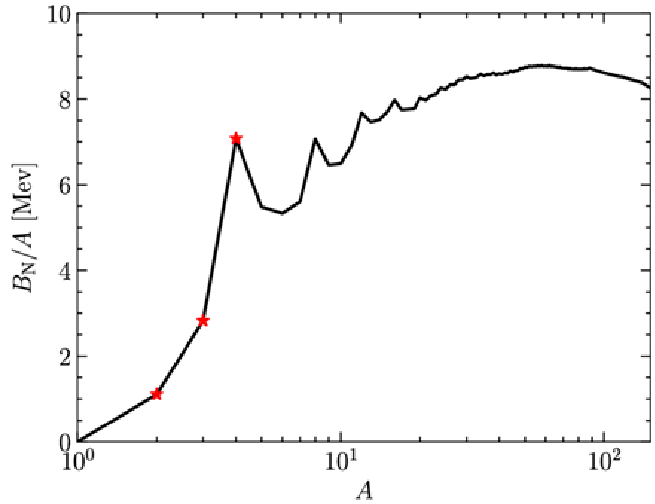

Figure 3. Binding energy per nucleon with D, T, and ^{4}He marked. From S. Dodelson & F. Schmidt (2020).

We note that $\dot{x} = -Q\dot{T}/T^2 = -x\dot{T}/T^2$ and since $T \propto a^{-1}$ (see Chapter 1), it follows that

$$\frac{1}{T}\frac{\mathrm{d}T}{\mathrm{d}t} = a\frac{\mathrm{d}a^{-1}}{\mathrm{d}t} = -\frac{1}{a}\frac{\mathrm{d}a}{\mathrm{d}t} = -H = -\sqrt{\frac{8\pi G\rho}{3}}\,. \tag{3.9}$$

Since during early times the universe is radiation-dominated, the contribution to energy density from relativistic particles is[9]

$$\begin{aligned}\rho &= \frac{\pi^2}{30}T^4\left[\sum_{i=\text{bosons}} g_i + \frac{7}{8}\sum_{i=\text{fermions}} g_i\right] \\ &= g_*\frac{\pi^2}{30}T^4\,,\end{aligned} \tag{3.10}$$

we have that $H \propto \sqrt{\rho} \propto T^2 \propto x^{-2}$, so $H(x=1) = x^2 H(x)$. Going back to (3.7):

$$\frac{\mathrm{d}X_n}{\mathrm{d}x} = \frac{x\lambda_{np}}{H(x=1)}\left[e^{-x} - X_n(1+e^{-x})\right]\,, \tag{3.11}$$

with

$$H(x=1) = Q^2\sqrt{\frac{4\pi^3 G}{45}g_*} \simeq 1.13\,\mathrm{s}^{-1}\,. \tag{3.12}$$

We also need an expression for the neutron-proton conversion rate (J. Bernstein et al. 1989):

$$\lambda_{np} = \frac{255}{\tau_n x^5}(12 + 6x + x^2)\,, \tag{3.13}$$

the neutron lifetime being $\tau_n = 878.4\,\mathrm{s}$. We can quickly estimate the conversion rate at $T = Q$ (i.e. $x = 1$) which turns out to be $5.5\,\mathrm{s}^{-1}$, slightly larger than the expansion rate above. However, as we shall see, under temperatures of 1 MeV the rate falls rapidly below the expansion rate, therefore rendering the reactions inefficient and effectively stopping this channel of neutron depletion.

We can estimate the freeze-out temperature as follows. The neutron-proton interconversion rate per nucleon is $\Gamma_{n\leftrightarrow p} \sim G_{\rm F}^2 T^5$; on the other hand, the expansion rate is $H \sim \sqrt{g_* G_{\rm N}}\,T^2$, where $G_{\rm F}$ and $G_{\rm N}$ are Fermi's and Newton's constants respectively. Equilibrium is lost when the conversion rates drops below the expansion rate, which happens

[9] The effective number of relativistic degrees of freedom, g_* in general depends on temperature. However, if we only take into account relativistic particles, photons contribute with $g_\gamma = 2$ (for two polarizations), neutrinos have $g_\nu = 6$ (three generations of neutrinos and antineutrinos with one spin degree of freedom each), and for electrons and positrons, $g_{e^-} = g_{e^+} = 2$. Adding up, $g_* \simeq 10.75$.

around $T_{\rm fr} \sim (g_* G_{\rm N}/G_{\rm F}^4)^{1/6} \simeq 1\,{\rm MeV}$. After freeze-out, neutrons continue to decay until nuclear reactions begin, further reducing their fraction.

A more accurate treatment of neutron abundance evolution requires solving the differential equation

$$\frac{{\rm d}X_n}{{\rm d}t} = -\lambda_{np} X_n + \lambda_{pn}(1 - X_n)\,, \tag{3.14}$$

with λ_{np} and λ_{pn} being time/temperature dependent reaction rates which are calculated from considering weak interactions. For example, the reaction rate for neutron decay is given by the approximate formula:

$$\Gamma = \frac{1}{(4\pi)^3 m_n} \int |\mathcal{M}|^2 (1 - f_\nu)(1 - f_e)\,{\rm d}E_e\,{\rm d}E_\nu\ . \tag{3.15}$$

Here $|\mathcal{M}|^2$ is the squared matrix element for the relevant reaction, f is the distribution function (in this case Fermi-Dirac), and the factors $(1-f)$ correspond to Pauli blocking for produced leptons (if a lepton is produced in a reaction, it cannot go into a state that is already occupied by an existing lepton). What can be done to simplify these is to normalize them to, say, continuing the example, the inverse of the neutron lifetime. We can also check that the direct and inverse rates calculated in this way respect the detailed balance principle.

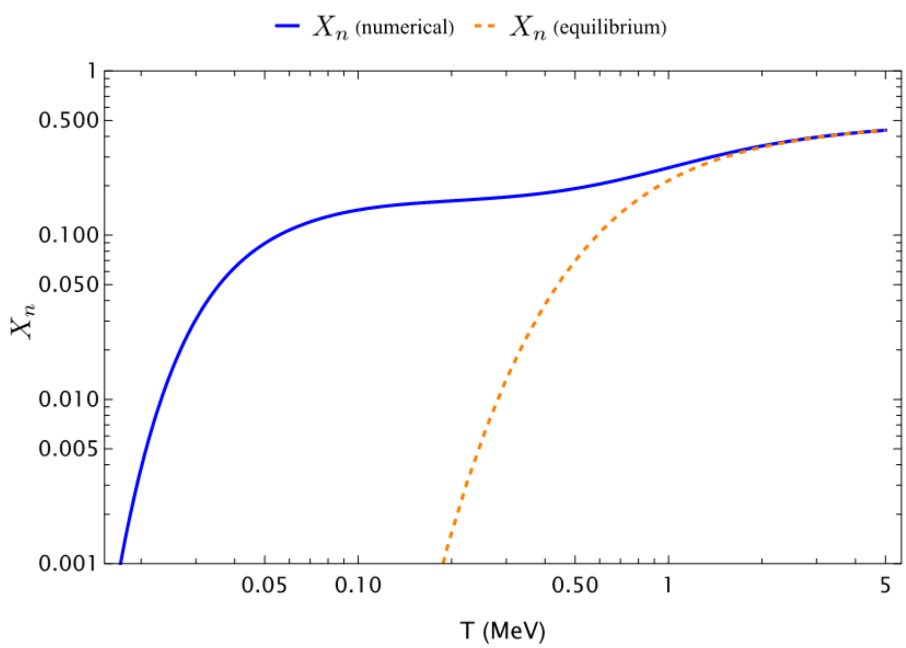

Figure 4. The evolution of neutron abundance with temperature in the early universe.

In Fig. 4 (obtained after solving the differential equation numerically), we can clearly see neutron freeze-out happen at around 1 MeV, as the line departs from the equilibrium abundance. It briefly freezes out at roughly 0.15 once the temperature drops below 0.5 MeV. As the temperature drops, the neutron-proton reactions fall out of equilibrium. After neutron freeze-out the only reaction that appreciably changes the number of neutrons is neutron decay. Without further reactions to preserve neutrons within stable nuclei, the universe today would be essentially pure hydrogen. The reaction that preserves neutrons is deuterium formation.

It is an amazing coincidence that neutron freeze-out temperature and the mass difference Q almost coincide. If this were not the case, the universe would look much different today. This property would not hold if the masses of u- and d-quarks, or the Fermi constant, or Newton's gravity constant were different from what they are. Due to this "coincidence", the neutron abundance at freeze out is rather large, so the abundances of light nuclei are considerable in the end: if it turned out that $Q \gg T_n$, then the neutron abundance at freeze-out would be exponentially small. On the other hand, for $Q \ll T_n$, neutrons and protons would be equally abundant at freeze-out, so all of them would end up in ^{4}He nuclei and the primordial plasma would lack hydrogen – such a hydrogen-free universe would hardly be habitable.

3.2. *Nuclei formation*

We are now ready to move to nuclei formation. Looking back at Fig. 3, we know that for a system in equilibrium, all nucleons should fuse into iron which has the highest binding energy per nucleon. However, due to the expansion of the universe, most nuclear reaction rates will fall well below the expansion rate before this can happen and will cease to be effective. By the time the temperature falls to below 0.1 MeV, the reaction rates are too low to produce heavier elements. Furthermore, since there exists no stable isotope with $A = 5$ and $A = 8$, only nuclei up to helium will be produced with considerable abundances, and others such as ^{7}Li or ^{7}Be with only trace abundances.

^{4}He is a very distinct peak in the graph in Fig. 3, which means that protons and neutrons have a strong tendency to form it. However, such a four-body interaction is very unlikely, so forming helium-4 requires the intermediate step of forming deuterium first. However, there is a caveat -– the temperature at this time is not much lower than the binding energy of deuterium and, given that photons are a billion times more numerous than baryons, there are sufficient photons with high enough energies to instantly destroy newly formed deuterium. We thus have to wait until the temperature has fallen sufficiently for a substantial concentration of D to build up before nucleosynthesis can continue. This is sometimes referred to as the *deuterium bottleneck*. It essentially means that the formation of helium-4 was delayed until the universe became cool enough for deuterium to survive (at about $T = 0.1$ MeV), after which there was a sudden burst of element formation.

^{12}C is another important peak but cannot be produced in two body reactions (not enough ^{6}Li), and reactions of more than two nuclei are extremely unlikely. This is why the chain does not reach carbon in the early universe. In stars, the bottleneck is bypassed by triple collisions of helium-4 nuclei, producing carbon (the triple-alpha process). However, this process is very slow and requires much higher densities than the ones available at this point in the universe.

Once neutrons become bound in nuclei, they become stable. This means that all neutrons from the early universe either decay away or become bound in light nuclei. Virtually all available neutrons are used to produce ^{4}He, so its abundance is only limited by the number of neutrons in the plasma. Some deuterium does remain though, as we will see, simply because the reaction that eliminates it is not completely efficient. In other words, the expansion of the universe cut the conversion short before it could proceed to the end. Taking the abundance of neutrons from the graph in Fig. 4 at, say, 0.08 MeV, and using a simple counting argument (two neutrons go into one ^{4}He) gives an abundance of helium of around 25%, which roughly matches observations.

We would of course like to be more rigorous than this. With regard to that, it is necessary to consider all the following nuclear reactions:

$$
\begin{aligned}
p + n &\to \mathrm{D} + \gamma & \qquad {}^3\mathrm{He} + n &\to \mathrm{T} + p \\
D + p &\to {}^3\mathrm{He} + \gamma & \mathrm{T} + p &\to {}^4\mathrm{He} + \gamma \\
\mathrm{D} + \mathrm{D} &\to {}^3\mathrm{He} + n & \mathrm{T} + \mathrm{D} &\to {}^4\mathrm{He} + n \\
\mathrm{D} + \mathrm{D} &\to \mathrm{T} + p & {}^3\mathrm{He} + \mathrm{D} &\to {}^4\mathrm{He} + p \\
{}^3\mathrm{He} + n &\to \mathrm{T} + p & \mathrm{T} + {}^4\mathrm{He} &\to {}^7\mathrm{Li} + \gamma \\
\mathrm{T} + p &\to {}^4\mathrm{He} + \gamma & {}^3\mathrm{He} + {}^4\mathrm{He} &\to {}^7\mathrm{Be} + \gamma \\
\mathrm{D} + \mathrm{D} &\to {}^3\mathrm{He} + n & {}^7\mathrm{Be} + n &\to {}^7\mathrm{Li} + p \\
\mathrm{D} + \mathrm{D} &\to \mathrm{T} + p & {}^7\mathrm{Li} + p &\to 2\,{}^4\mathrm{He}
\end{aligned}
$$

as well as the corresponding inverse reactions. We therefore have 8 ingredients (not counting photons) and 24 nuclear reactions. It is relatively straightforward to write the differential equations governing the change in abundances of each of them, simply by taking rates for all nuclear reactions where the nucleus of interest shows up. For example, the equation for neutron abundance is now as follows:

$$\dot{X}_n = -(n \to p)X_n + (p \to n)X_p \tag{3.16}$$
$$- (n\,p \to \mathrm{D}\,\gamma)X_n X_p n_\mathrm{b} + (\mathrm{D}\,\gamma \to n\,p)X_\mathrm{D} X_\gamma n_\mathrm{b} \tag{3.17}$$
$$+ (\mathrm{D}\,\mathrm{D} \to {}^3\mathrm{He}\,n)\frac{1}{2}X_\mathrm{D} X_\mathrm{D} n_\mathrm{b} - ({}^3\mathrm{He}\,n \to \mathrm{D}\,\mathrm{D})X_{^3\mathrm{He}} X_n n_\mathrm{b} \tag{3.18}$$
$$- ({}^3\mathrm{He}\,n \to \mathrm{T}\,p)X_{^3\mathrm{He}} X_n n_\mathrm{b} + (\mathrm{T}\,p \to {}^3\mathrm{He}\,n)X_\mathrm{T} X_p n_\mathrm{b} \tag{3.19}$$
$$+ (\mathrm{T}\,\mathrm{D} \to {}^4\mathrm{He}\,n)X_\mathrm{T} X_\mathrm{D} n_\mathrm{b} - ({}^4\mathrm{He}\,n \to \mathrm{T}\,\mathrm{D})X_{^4\mathrm{He}} X_n n_\mathrm{b} \tag{3.20}$$
$$- ({}^7\mathrm{Be}\,n \to {}^7\mathrm{Li}\,p)X_{^7\mathrm{Be}} X_n n_\mathrm{b} + ({}^7\mathrm{Li}\,p \to {}^7\mathrm{Be}\,n)X_{^7\mathrm{Li}} X_p n_\mathrm{b}\,, \tag{3.21}$$

and similarly for other nuclei. Notice the factor of 1/2 in the third line which appears because of the fact that the reaction uses two deuterium nuclei. In general, the evolution of abundances with arbitrary nuclear reactions $i_1 \dots i_p \to j_1 \dots j_q$ take the form (C. Pitrou et al. 2018):

$$\dot{X}_{i_1} = \sum_{i_2,\dots,i_p,j_1,\dots,j_q} N_{i_1} \left(\Gamma_{j_1\dots j_q \to i_1 \dots i_p} \frac{X_{j_1}^{N_{j_1}} \dots X_{j_q}^{N_{j_q}}}{N_{j_1}! \dots N_{j_q}!} - \Gamma_{i_1\dots i_p \to j_1 \dots j_q} \frac{X_{i_1}^{N_{i_1}} \dots X_{i_p}^{N_{i_p}}}{N_{i_1}! \dots N_{i_p}!} \right) \tag{3.22}$$

where N_i is the stoichiometric coefficient of species i in the reaction. The rates Γ appearing in the formula above are related to number density rates by

$$\Gamma_{i_1\dots i_p \to j_1 \dots j_q} = n_\mathrm{b}^{(N_{i_1}+\dots+N_{i_p})-1} \gamma_{i_1\dots i_p \to j_1 \dots j_q} \tag{3.23}$$

and

$$\gamma_{i_1\dots i_p \to j_1 \dots j_q} \equiv \langle \sigma v \rangle_{i_1\dots i_p \to j_1 \dots j_q} \tag{3.24}$$

are really the thermally averaged cross sections.

Finally, the inverse reactions are related to the direct ones through (C. Pitrou et al. 2018):

$$\frac{\gamma_{j_1\dots j_q \to i_1 \dots i_p}}{\gamma_{i_1\dots i_p \to j_1 \dots j_q}} = \frac{\prod_{i=i_1,\dots,i_p} \frac{1}{N_i!} \left[g_i \left(\frac{m_i T}{2\pi} \right)^{3/2} \right]^{N_i}}{\prod_{j=j_1,\dots,j_q} \frac{1}{N_j!} \left[g_j \left(\frac{m_j T}{2\pi} \right)^{3/2} \right]^{N_j}} \exp\left(\frac{\sum_{j=1}^q m_j - \sum_{i=1}^p m_i}{T} \right). \tag{3.25}$$

The quantity in the numerator of the exponent is nothing but the energy released or absorbed in a certain reaction.

After including the relevant nuclear reactions and solving the system of coupled differential equations for the abundances of all nuclei simultaneously, we obtain the graph shown in Fig. 5. The evolution of all the main isotopes is plotted as a function of time and temperature. For reference, the following sequence of events occurs during BBN: (a) the chemical decoupling of neutrinos from the thermal bath (2–3 MeV, not shown in graph), (b) the annihilation of electrons and positrons, (c) the freeze-out of neutrons and protons (1 MeV, not shown in graph), (d) an "intermission" between that and the deuterium ignition at the end of the "bottleneck," (e) helium synthesis at around 70 keV, and finally (f) a follow-up stage in which the main nuclear reactions gradually drop out of equilibrium and the abundances of all light elements freeze out. Of course, after this unstable nuclei will continue to decay – these are shown with dashed lines, with T decaying to ^{3}He and ^{7}Be to ^{7}Li.

The results match previous studies well, such as C. Pitrou et al. (2018), which in turn match astronomical observations. Generally speaking (with the exception of the lithium problem), there is good agreement between theory and experiment here. Astronomically, the abundances are usually measured in the intergalactic medium and low-metallicity gas clouds. Spectroscopic measurements of relative local element abundances are quite precise by themselves. The major uncertainties are systematic and, roughly speaking, have to do with limited confidence on the primordial origin of these abundances. The abundances remained unchanged until first stars formed. Then, heavier elements were synthesized, and some fragile primordial ones could be destroyed (especially deuterium).

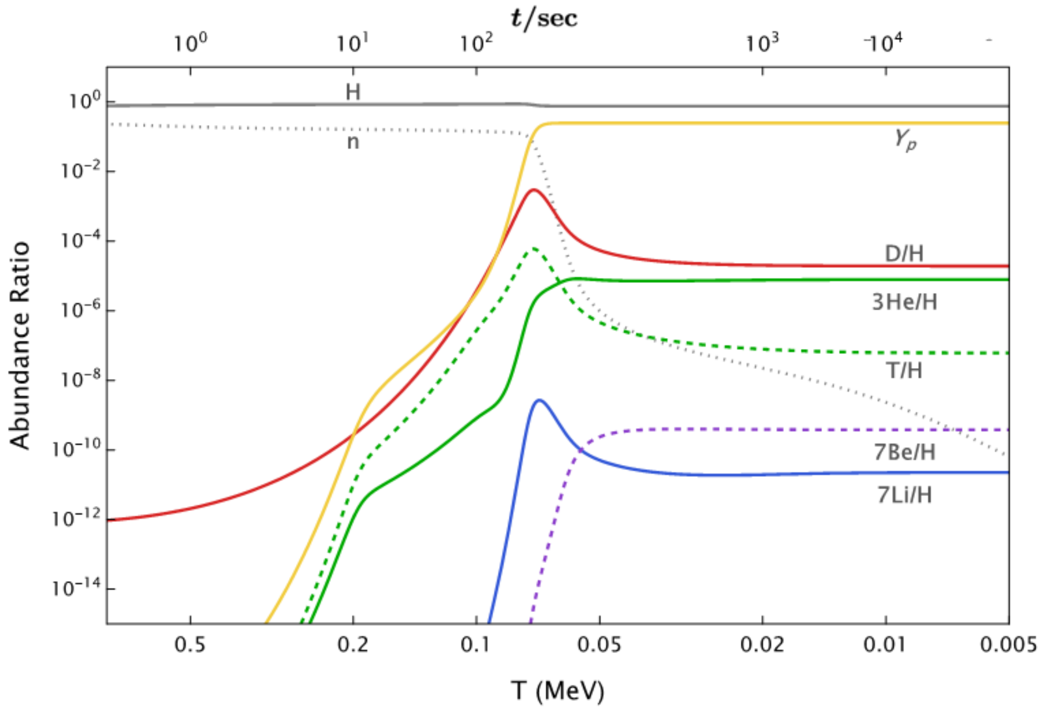

Figure 5. Evolution of abundances of light nuclei during BBN. All abundances are shown relative to H (protons), except for ^{4}He, for which it is customary to plot the mass abundance $Y_p = 4X_{^4\mathrm{He}}$.

3.3. *Dependence of abundances on the baryon-to-photon ratio and relevant nuclear reaction rates*

As already mentioned, the baryon-to-photon ratio is known with very good precision from CMB observations, a measurement completely independent from BBN (Eq. 3.4). Nevertheless, it is interesting to see how variations in this parameter influence some abundances. In this section, we focus only on deuterium and helium-4 which serve as nice examples of very different dependences.

We vary η_b by $\pm 1\%$ and fit the calculated points at several points to a power law. We also do the same for reaction rates, the most influential ones being $\mathrm{D} + \mathrm{D} \to {}^3\mathrm{He} + n$ and $\mathrm{D} + \mathrm{D} \to \mathrm{T} + p$. The results for D and ^{4}He are:

$$\frac{\mathrm{D}}{\mathrm{H}} = 2.538 \cdot 10^{-5} \left(\frac{\eta_b}{6.109 \cdot 10^{-10}}\right)^{-1.633} \left[\mathrm{D}(\mathrm{D}, n)^3\mathrm{He}\right]^{-0.547} \left[\mathrm{D}(\mathrm{D}, p)\mathrm{T}\right]^{-0.453} \tag{3.26}$$

$$Y_p = 0.246 \left(\frac{\eta_b}{6.109 \cdot 10^{-10}}\right)^{0.039} \left[\mathrm{D}(\mathrm{D}, n)^3\mathrm{He}\right]^{0.006} \left[\mathrm{D}(\mathrm{D}, p)\mathrm{T}\right]^{0.005} \tag{3.27}$$

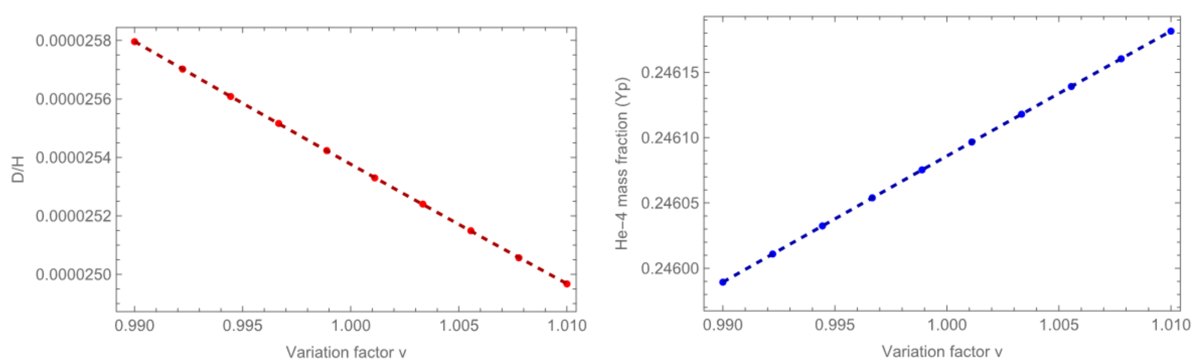

Figure 6. Dependence of deuterium and helium-4 abundances on variations to the baryon-to-photon ratio.

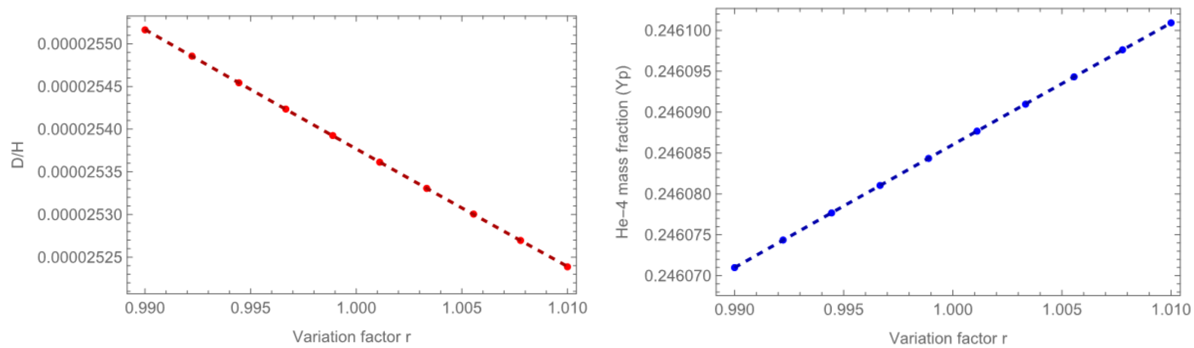

Figure 7. Dependence of deuterium and helium-4 abundances on variations to the rate of the reaction $\mathrm{D}+\mathrm{D}\rightarrow {}^{3}\mathrm{He}+n$

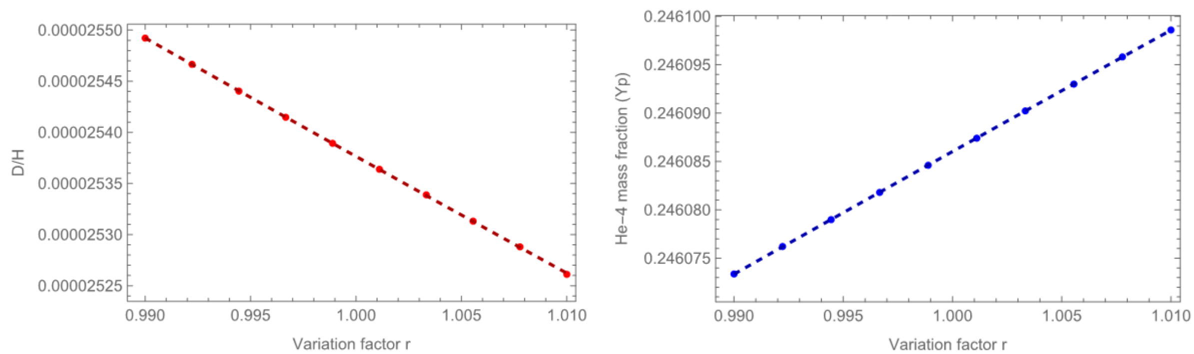

Figure 8. Dependence of deuterium and helium-4 abundances on variations to the rate of the reaction $\mathrm{D}+\mathrm{D}\rightarrow \mathrm{T}+p$

We can notice strong dependences in the deuterium abundance and very weak ones when it comes to helium-4. The negative powers for deuterium are easily explained. For the reaction rates, it is obvious that, the more efficient these two reactions are, the more deuterium gets processed. However, as we have seen from Fig. 5, not all of the deuterium gets processed into helium. A trace amount remains unburned, simply because the reactions that eliminate it are not completely efficient. While deuterium is depleted via these reactions, it eventually freezes out at a mass fraction of order $3\cdot 10^{-5}$ due to the expansion that cooled the universe and reduced the density, which cut the conversion short before it could proceed any further.

The dependence on the baryon-to-photon ratio is explained as follows. The denser the initial universe was (or the more baryons there were), the more deuterium would be converted to helium-4 before time ran out, and the less deuterium would remain. If the baryon density is lower, then the reactions proceed more slowly, and the depletion is not as effective. Therefore, low baryon density inevitably results in more deuterium. One consequence of this is that, unlike helium-4, the amount of deuterium is very sensitive to initial conditions.

BBN actually predicts a primordial abundance of about 25% helium-4 by mass, irrespective of the initial conditions of the universe (there is a weak logarithmic dependence on the baryon number ratio). As long as the universe was hot enough for protons and neutrons to transform into each other easily, their ratio, determined solely by their relative masses, was about 1 neutron to 7 protons. One analogy is to think of helium-4 as ash: the amount of ash that we get when we completely burn a piece of wood is insensitive to how we burn it.

A potential next step, apart from examining the dependence on other reaction rates in the same fashion, could be to introduce a temperature/energy-dependent variation. In other words, instead of scaling the reaction rate over the entire energy range by the same factor, it would be interesting to only introduce some variation in a certain energy range. This would allow to examine which energy ranges are most critical and influential for the abundances. With this knowledge, one could determine critical energy ranges in which more accurate rate measurements are needed to improve theoretical knowledge of the abundances (especially for deuterium). By doing this, we can hope to allow stronger cosmological inferences to be made from BBN-related observations, such as restrictions on N_{eff}.

ACKNOWLEDGMENTS

I thank my supervisors Miguel Escudero Abenza and Maksym Ovchynnikov for their guidance and support during the work on this project. I have learned from them much more than I could have hoped in this short time. I would also like to thank all the other researchers and employees at the Theory Department who have made me feel comfortable and inspired every day, many of whom especially helped me with discussions and useful suggestions regarding my project. Finally, I thank my summer student friends at CERN, working in many different fields and at various collaborations, for providing me with unforgettable memories and experiences during these summer months. Thank you to the CERN Summer Student Team for selecting me for this incredible opportunity. I am beyond grateful for having the chance to learn and explore more about our vast and amazing universe in such an awe-inspiring place like CERN.

APPENDIX

A. NATURAL UNITS

Throughout these notes, we use natural units as is standard practice in cosmology:

$$\hbar = c = k_{\mathrm{B}} = 1. \tag{A1}$$

For example, a temperature of approximately 11600 K corresponds to 1 eV.

REFERENCES

Bernstein, J., Brown, L. S., & Feinberg, G. 1989, Rev. Mod. Phys., 61, 25, doi: 10.1103/RevModPhys.61.25

Brout, D., Scolnic, D., Popovic, B., et al. 2022, The Astrophysical Journal, 938, 110, doi: 10.3847/1538-4357/ac8e04

Cooke, R. J., Pettini, M., & Steidel, C. C. 2018, Astrophys. J., 855, 102, doi: 10.3847/1538-4357/aaab53

Dodelson, S., & Schmidt, F. 2020, Modern Cosmology (Academic Press), doi: 10.1016/C2017-0-01943-2

Fixsen, D. J. 2009, The Astrophysical Journal, 707, 916–920, doi: 10.1088/0004-637x/707/2/916

Fixsen, D. J., Cheng, E. S., Gales, J. M., et al. 1996, Astrophys. J., 473, 576, doi: 10.1086/178173

Pitrou, C., Coc, A., Uzan, J.-P., & Vangioni, E. 2018, Physics Reports, 754, 1–66, doi: 10.1016/j.physrep.2018.04.005

Rubakov, V. A., & Gorbunov, D. S. 2017, Introduction to the Theory of the Early Universe: Hot big bang theory (Singapore: World Scientific), doi: 10.1142/10447